Measurement of Cognitive and Kinematic Adaptation in Exoskeleton-Assisted Locomotion: Validation of an XR-Based Framework

Nicola Abeni *, Riccardo Costa, Emilia Scalona, Diego Torricelli, Matteo Lancini

Posted Date: 14 April 2026

doi: 10.20944/preprints202604.0925.v1

Keywords: measurements; exoskeleton; kinematics; cognitive load; visuospatial attention; rehabilitation; mixed reality; wearable sensors; eye-tracking; assisted locomotion

 doi:10.20944/preprints202604.0925.v1

Article

Measurement of Cognitive and Kinematic Adaptation in Exoskeleton-Assisted Locomotion: Validation of an XR-Based Framework

Nicola Abeni [1,*], Riccardo Costa [1], Emilia Scalona [2], Diego Torricelli [3] and Matteo Lancini [4]

[1] Department of Mechanical and Industrial Engineering, University of Brescia, Italy
[2] INAIL Prosthetic Centre, Vigorso di Budrio, Bologna, Italy
[3] BioRobotics group, Centre for Automation and Robotics (CAR), CSIC, Madrid, Spain
[4] Department of Medical and Surgical Specialties, Radiological Sciences, and Public Health, University of Brescia, Italy
* Correspondence: nicola.abeni@unibs.it

Abstract

Robotic assistive devices, such as exoskeletons, are increasingly employed in walking rehabilitation. Therefore, the measurement of both movement kinematics and cognitive workload is important to understand this human-robot interaction in real-world contexts. To address this need this study presents the validation of a framework integrating inertial motion capture (Xsens) and eye-tracking sensor (Pupil Neon) within a Mixed Reality (Meta Quest 3) architecture. We developed an overground dual-task paradigm in which holographic numbers appear in the user's peripheral vision. This setup actively stimulates visuospatial attention while quantifying kinematic and cognitive output. To validate the framework, the protocol has been tested on 30 healthy subjects across repeated exoskeleton training sessions. Statistical analyses revealed that the Multiple Correlation Coefficient (CMC) and Spectral Arc Length (SPARC), calculated on the shank angular velocity, together with the Step Length Variability exhibited significant time effects ($p < 0.01$), mapping the transition toward automated gait. Concurrently, pupillometric data demonstrated a measurable reduction in neurocognitive demand; specifically, the Task-Evoked Pupillary Response (TEPR) decreased significantly across progressive training sessions ($p < 0.05$). With this work, we validated a measurements protocol that aims to provide a novel methodology for objectively evaluating motor and cognitive adaptation in wearable assistive devices.

Keywords: measurements; exoskeleton; kinematics; cognitive load; visuospatial attention; rehabilitation; mixed reality; wearable sensors; eye-tracking; assisted locomotion

1. Introduction

The ability to move freely is essential for performing everyday tasks. This significantly influences human life quality, well-being, and social engagement. However, injuries such as spinal cord injuries (SCI), neurological disorders, stroke and cerebral palsy can severely limit walking mobility. Consequently, the demand for assistive technology is increasing [1], leading to a growing interest in advanced devices. Over the past decade, the research on robotic exoskeletons has experienced significant growth. Hardware and energy sources have been improved and has lead to the development of functional prototypes suitable for human testing [2,3]. Nowadays, lower-limb exoskeletons are generally divided into three categories: the ones which are designed to enhance the physical capabilities of able-bodied individuals; those which enable people with disabilities to accomplish movements they cannot do independently; and therapeutic exoskeletons used for rehabilitation to help, resist or perturb the user's movements [3]. Traditionally, it is the experience of the physicians that assesses the training during rehabilitation processes with these devices. In addition to that, kinematics and force measurements

 doi:10.20944/preprints202604.0925.v1

have gained prominence as objective tools to support clinical evaluation. While these physical metrics are essential, relying solely on them leaves an evaluation gap regarding the user's cognitive load [4]. In fact, although exoskeletons continue to evolve in terms of mechanical sophistication and effectiveness, their widespread and long-term adoption remains limited. The major obstacle hindering their daily use is no longer just physical, but regards the high mental workload involved [5]. Even if there is a plurality of definitions about what mental workload is , we opt for the one related to the field of human-robot interaction, including the wearable assistive devices, as the exoskeletons. That's why this cognitive effort could be described as "the amount of demand placed on the user by the system" [6]. Walking is typically an automatic activity for able-bodied individuals, while operating a powered exoskeleton necessitates a significant concentration level, requiring focus at each step [7]. This heightened cognitive demand restricts the user from navigating uneven surfaces and hinders the ability to engage in concurrent activities, such as holding a conversation or processing complex visual information from the surroundings [6–8]. Within this context, visuospatial attention is a critical component during exoskeleton-assisted locomotion [9,10]. The high cognitive demand of operating an exoskeleton can saturate the user's limited neural resources, impairing their ability to scan the environment and increasing fall risks [11,12]. Under these conditions of cognitive overload, a phenomenon known as "inattentional blindness" [13] is often triggered: the brain becomes so absorbed by the primary task that it ceases to consciously process visual information. Consequently, users may physically direct their gaze straight to an obstacle or hazard without actually perceiving or registering its presence. Because of this discrepancy between mechanical gaze orientation and actual conscious perception, relying on metrics that only track eye direction is insufficient to quantify true cognitive effort. A robust assessment of true mental workload therefore, requires the integration of active visuospatial paradigms capable of measuring actual attentional engagement in parallel with physical performance. A notable example that successfully addresses the issue of inattentional blindness through target-distractor differentiation is the Standing and Walking Visual Attention Field (SWAVF) task [9]. This SWAVF task has been developed to evaluate covert visuospatial attention during locomotion. It requires users to maintain a forward gaze while actively scanning the lower peripheral visual field. During the walk, participants are prompted to identify a specific target hidden among several distractors (e.g., differentiating a yellow light from multiple green lights) and must make a deliberate behavioral response to indicate the target's location. By forcing this active target-distractor differentiation and a physical reaction to the stimuli, the SWAVF paradigm guarantees that the visual information was successfully and consciously processed. However, while this paradigm is highly effective, it was originally validated exclusively during seated and unassisted walking, without the inclusion of any robotic device. Furthermore, its physical setup is inherently confined to treadmill-based walking. Together, these factors restrict the evaluation to controlled laboratory setups and prevent a truly ecological assessment of human-robot interaction in overground scenarios. This specific gap is reflected in the broader literature, where only a small fraction of cognitive assessment studies (approximately 20%) focus on exoskeletons compared to prostheses. To overcome traditional limitations, recent research has explored advanced technologies to assess human-robot interaction; however, these tools are typically applied in isolation. For instance, eye-tracking and pupillometry have been adopted to evaluate the cognitive burden associated with prosthetic hands [14] and lower-limb exoskeletons [15,16], whereas Augmented and Virtual Reality (AR/VR) paradigms have been primarily restricted to static industrial tasks or upper-limb rehabilitation [17–19]. Furthermore, although international benchmarking initiatives (e.g., EUROBENCH) have made strides in standardizing the combined measurement of biomechanical and physiological data during exoskeleton use, they lack immersive, visually engaging settings [20]. To the best of our knowledge, no existing research has combined dual-task paradigms, extended reality (XR), kinematics, and eye-tracking measurements to evaluate exoskeleton-assisted locomotion. Furthermore, there remains a critical need for measurement frameworks capable of integrating these metrics to simultaneously assess physical performance and cognitive workload in ecological settings [21]. To address this literature gap, this study presents the metrological validation of a novel measurement protocol that

 doi:10.20944/preprints202604.0925.v1

aims to objectively assess the exoskeleton-assisted locomotion. The proposed framework integrates an IMU-based motion capture system (Xsens MTw Awinda) with wearable eye-tracking technology (Pupil Neon) embedded within a Mixed Reality (XR) headset (Meta Quest 3). This configuration enables users to perform overground walking while navigating a holographic environment, facilitating an ecological evaluation of motor progress while actively stimulating visuospatial attention. Specifically, the concurrent cognitive task requires participants to visually identify, fixate upon, and verbally report a green number appearing in their peripheral field of view. To intentionally increase the cognitive demand, participants were instructed to report the number in English, which was not their primary language. Through this setup, the main objective of this work is to demonstrate that the system is sensitive enough to monitor the training process. We focus on capturing both kinematic progress and the associated cognitive demand as users adapt to the device, establishing a practical framework for assessing how humans and robotic devices work together.

2. Materials and Methods

The experimental framework (Figure 1) evaluates motor and cognitive adaptation during exoskeleton-assisted walking through a novel dual-task paradigm. Thirty healthy participants performed overground walking with a lower-limb exoskeleton (Exo-H3) while simultaneously engaging in a mixed-reality visual search task (Meta Quest 3). Kinematic stability (Xsens IMUs) and cognitive workload (Pupil Neon eye-tracking) were continuously monitored across repeated training sessions to objectively quantify the learning process and the human-robot interaction.

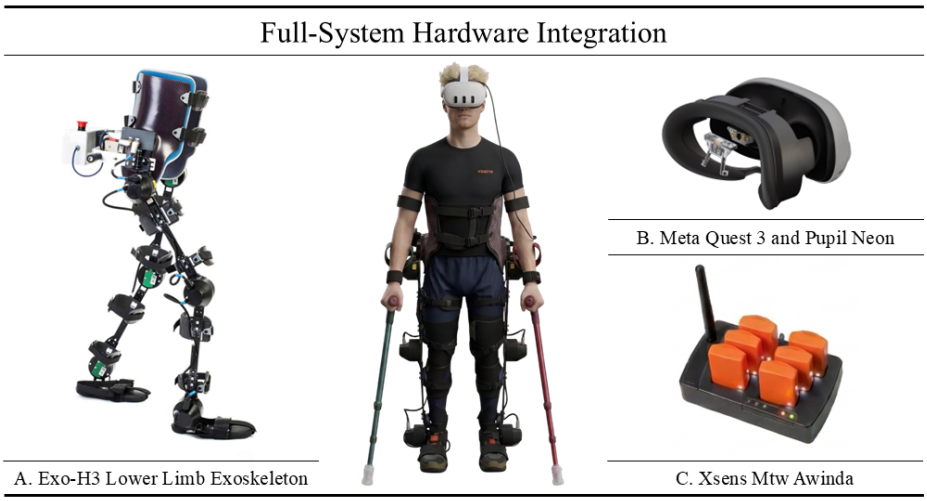

Figure 1. Overview of the integrated multi-modal experimental setup. The complete on-body setup worn by a user includes: (A) Exo-H3 lower limb exoskeleton; (B) Meta Quest 3 headset with Pupil Neon eye-tracking; and (C) Xsens MTw Awinda inertial sensors.

2.1. Materials

The Exo-H3 lower-limb exoskeleton (Technaid S.L., Madrid, Spain) developed in collaboration with the CSIC Neurorehabilitation group, has been used to safely replicate a rehabilitation scenario in this study with healthy subjects. This device provides six degrees of freedom in the sagittal plane, assisting the flexion and extension of the hips, knees, and ankles for both legs.

The wireless MTw Awinda system (Xsens Technologies B.V., Enschede, The Netherlands) has been adopted to record users' movement and accurately extract the full-body kinematics through the MVN Analyze software [22]. This setup uses 17 synchronized inertial measurement units (IMUs) operating at a sampling frequency of up to 60 Hz.

Furthermore, the system integrates a Meta Quest 3 (Meta Platforms, Inc., Menlo Park, CA, USA) to administer the cognitive task in Mixed Reality (MR) and Pupil Neon glasses (Pupil Labs GmbH, Berlin, Germany) to monitor visual attention and pupillometry. The headset's RGB cameras and depth

 doi:10.20944/preprints202604.0925.v1

sensors allow for the overlay of virtual elements onto the physical world, ensuring safe navigation. Moreover, the eye tracker streams real-time gaze data to the Meta headset via the Neon XR Core Package.

Finally, the dual-task application was developed using Unity v2022.3.62f2 (Unity Technologies, San Francisco, CA, USA). All the data analysis has been carried out using Matlab (The MathWorks, Inc., Natick, MA, USA) and executed on a Dell XPS 9520 with a Intel Core i7-12700H @ 2.30 GHz processor.

2.2. Dual-Task Design

The cognitive activity designed to measure visuospatial attention was developed using the Standing and Walking Visual Attention Field (SWAVF) [9] task as a foundational concept. The original SWAVF task relies on a physical LED platform, involves walking on a treadmill, and forces participants to maintain their gaze on a fixed central point. Our custom version, instead, projects the task directly through the headset, allowing the subject to view the real world and freely move. This design eliminates the need to walk on a treadmill or to fixate the gaze on a specific location, thereby enabling natural visual exploration.

The trial begins by verifying the eye-tracker communication with the Meta headset. Participants observe two virtual white spheres reflecting their real-time gaze. The experiment proceeds upon the vocal confirmation. After this phase, the subject is instructed to perform specific head movements (nodding and shaking the head). This action generates a distinct kinematic signature across the data streams, serving as a backup mechanism for the offline temporal synchronization of all the involved sensors.

Then the actual cognitive task (Figure 2) can formally start.

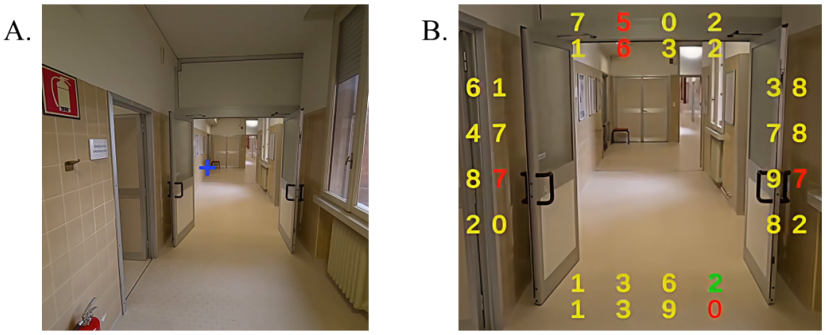

Figure 2. First-person perspective of the custom visuospatial attention task projected via the mixed-reality headset. (A) The trial cycle initiates with the presentation of a central blue cross. (B) Subsequently, a grid of colored numbers is displayed in the user's peripheral vision over the real-world environment. Participants must visually locate and verbally identify the single green target number (e.g., '2' in the bottom right) embedded among yellow numbers and red distractors.

The task operates cyclically, with trials repeating at randomized intervals of 2 to 4 seconds. Each cycle begins with a central blue cross (Figure 2A), immediately followed by a number grid in the user's peripheral vision (Figure 2B). This grid consists of yellow numbers, red distractors, and a single green target. Participants must visually locate the green target and read it aloud in English; using a non-native language serves to slightly elevate the cognitive demand. Furthermore, this verbal response replaces the manual clickers used in the original SWAVF task [9] to prevent inattentional blindness. This ensures conscious visual processing while avoiding any physical constraints. Since operating the exoskeleton requires the use of crutches for stability, holding and operating manual clickers would be highly impractical.

During the task, the application continuously logs the spatial positions and the exact appearance and disappearance timestamps of the target (green) and distractor (red) numbers. Additionally, the system records the user's real-time gaze coordinates within the virtual environment, their head position, and continuous audio of their vocal responses.

 doi:10.20944/preprints202604.0925.v1

2.3. Methods

2.3.1. Pupil Neon & Meta Quest 3 Gaze Calibration

A gaze calibration is needed to confirm that the user's gaze actually lands on the target number that is then verbally reported. In fact, the raw gaze data originates from the Pupil Neon sensor's local reference frame, while the holographic numbers exist within the Meta headset's 3D virtual coordinate system. Furthermore, the physical adapter holding the eye tracker can vary slightly in position and orientation depending on the user's facial anatomy. Therefore, a spatial transformation is required for each user to align these two distinct reference frames.

The calibration process uses the PL_Calibration scene, an official, pre-built tool provided by Pupil Labs as part of their Neon XR Unity package. The VR headset sequentially renders a series of visual markers at predefined, fixed 3D coordinates within the virtual environment. As the user focuses on each marker, the system continuously pairs the raw gaze vectors with the exact 3D position of the virtual target. Once a sufficient number of samples is collected, the software employs an iterative Kabsch algorithm to compute the optimal rigid body transformation. Specifically, it calculates the translation and rotation matrices that minimize the root-mean-square deviation (RMSD) between the projected gaze points and the actual target coordinates. The transformation matrix is then saved as a configuration file, which can be applied globally to convert real-time, raw gaze data into VR world-space rays.

2.3.2. Pupil Neon & Meta Quest 3 Synchronization

During the experimental sessions, eye-tracking data were acquired simultaneously through two parallel pipelines to maximize temporal resolution and ensure data redundancy. The Unity application, using the Pupil Neon XR Core package, exclusively recorded basic parameters, including the raw gaze position in pixels relative to the sensor, the gaze vector transposed into the 3D coordinate system of the Meta Quest 3 headset, and pupil diameter, at a sampling frequency of approximately 80 Hz. Concurrently, the Pupil Labs Companion device performed a high-frequency local recording (200 Hz). It is important to note that while the Quest application only saved data related to gaze and pupil diameter, the Companion device also extracted and stored a comprehensive set of advanced metrics, including blinks, saccades, and fixations.

Given that the two data streams were asynchronous and sampled at different frequencies, a two-phase synchronization procedure was developed based on the raw horizontal gaze position (X_{gaze}). Initially, the low-frequency signal (Quest) was upsampled via linear interpolation to match the timestamps of the high-frequency signal (Pupil). Subsequently, cross-correlation was calculated to obtain a preliminary estimate of the time delay (time lag).

To further align the two streams, this initial delay was used as the starting point in an iterative optimization algorithm. The optimal time delay (Δt) was computed by minimizing a cost function $J(\Delta t)$ based on the mean squared error (MSE) between the two signals:

$$J(\Delta t) = \frac{1}{K} \sum_{k=1}^{K} \left(x_{pupil}(t_k) - x_{quest}(t_k - \Delta t) \right)^2 \quad (1)$$

where K represents the total number of valid samples. This optimized temporal offset (Δt) was then globally applied to the entire dataset. This ensured that all the additional metrics recorded exclusively by the Pupil hardware (blinks, saccades, and fixations) were synchronized with the virtual reality environment generated by the Meta Quest.

The gaze position was chosen as the primary synchronization signal because the Meta Quest saves the same raw data stream originating from the Pupil sensor, differing only by network delay. However, to ensure system robustness against potential communication interruptions between Unity and the eye-tracker, a kinematic fallback strategy was implemented. In the absence of reliable shared ocular data, synchronization was performed using the inertial signals (IMUs) independently recorded by the Meta Quest 3 and the Pupil Neon. Unlike the shared gaze stream, these IMUs are physically

 doi:10.20944/preprints202604.0925.v1

distinct sensors subject to independent hardware drift and varying automatic calibration routines. That's why this strategy was strictly reserved as a backup procedure.

2.3.3. Event Detection & Step Segmentation

To ensure proper kinematic analysis, it was necessary to exclude intervals where the subject was stationary or turning at the end of the walking path. This was achieved by tracking significant changes in the signal of the knee sagittal flexion-extension angle, discarding inactive portions, and retaining only the steady-state walking segments. Subsequently, the preserved data required segmentation into stance and swing phases. To accomplish this, Heel Strike (HS) and Toe Off (TO) events were extracted using a semi-custom algorithm starting from the work presented by Grimmer M. et Al. in [23]. The algorithm initiates by identifying the local maxima of the knee sagittal angle. Operating in a discrete domain, let T_s represent the sampling time and k the frame index. The time series is denoted as $y(kT_s)$. A local maximum at index k is systematically found when the angular value strictly exceeds its immediate neighbors:

$$y((k-1)T_s) < y(kT_s) > y((k+1)T_s) \tag{2}$$

This condition successfully isolates all sampled local maxima. To filter these peaks and avoid false positives, the algorithm applies an expected average step duration threshold (approximately 2 seconds) and a minimum angular amplitude constraint of 30°. The continuous walking cycle is then segmented into distinct windows defined by consecutive peaks. Within each peak-to-peak window, specific HS and TO events are determined by analyzing zero-crossings in the shank angular velocity (representing the segment between the knee and ankle). The HS event is defined as the first instance where the angular velocity transitions from a negative to a positive value, provided this positive state is sustained for a minimum of 10 sampling intervals. To prevent anticipatory detection, the HS must occur at least 200 ms after the window's onset. Conversely, the TO event is identified when the shank angular velocity transitions from positive to negative, again requiring the new state to hold for at least 10 sampling intervals. A temporal constraint is applied to the TO detection, mandating that it must occur after 60% of the total window duration has elapsed. While these thresholds provide robust automated segmentation, the constraints can be dynamically adjusted to accommodate specific subject characteristics, and manual refinement is allowed in cases of excessive signal noise.

2.3.4. Kinematic Metrics

To prevent the high dimensionality and multiple-testing correction issues that can reduce statistical power in gait analysis, a targeted selection strategy was adopted. The analysis focused on three complementary metrics to evaluate movement fluency and gait quality under dual-task cognitive conditions: Step Length Variability (SLV), Spectral Arc Length (SPARC), and the Coefficient of Multiple Correlation (CMC).

Step Length Variability (SLV) serves as a sensitive indicator of motor stability, spatial asymmetry, and potential fall risk during exoskeleton-assisted walking [24,25]. It captures step-to-step fluctuations and is quantified as the coefficient of variation (CV). Defining μ as the mean step length and σ as the standard deviation of the step length, the CV is calculated as:

$$SLV = CV = \frac{\sigma}{\mu} \tag{3}$$

A lower SLV indicates reduced variability and a more stable, controlled gait, whereas a higher SLV reflects elevated step-to-step instability [26].

To assess the continuity and non-intermittent nature of motion, the Spectral Arc Length (SPARC) was computed. The SPARC is a smoothness metric derived from the frequency spectrum of a signal and remains robust against variations in walking speed. In this case the SPARC has been applied to the shank angular velocity. Defining ω_c as the cutoff frequency distinguishing normal from pathological

 doi:10.20944/preprints202604.0925.v1

movement, and $\hat{A}(\omega)$ as the normalized Fourier spectrum amplitude of the movement profile, SPARC is calculated as the negative arc length of this spectrum:

$$SPARC = -\int_0^{\omega_c} \sqrt{\left(\frac{1}{\omega_c}\right)^2 + \left(\frac{d\hat{A}(\omega)}{d\omega}\right)^2} d\omega \tag{4}$$

Smoother movements concentrate the frequency spectrum at lower frequencies, yielding less negative SPARC values, while more irregular or jagged movements produce more negative values [27,28].

Finally, waveform similarity between repeated kinematic signals, specifically, normalized shank angular velocity profiles, was evaluated using the Coefficient of Multiple Correlation (CMC) [29]. This dimensionless measure integrates the effects of vertical offset, curve shape, and amplitude scaling. Defined F as the number of frames in a gait cycle, N as the number of cycles, Y_{ij} as the value at frame j in cycle i, $\bar{Y}_j$ as the mean at frame j across all cycles, and $\bar{Y}$ as the grand mean of all values, the CMC is calculated as the square root of 1 minus the ratio of residual variance to total variance:

$$CMC = \sqrt{1 - \frac{\sum_{i=1}^{N}\sum_{j=1}^{F}(Y_{ij} - \bar{Y}_j)^2}{\sum_{i=1}^{N}\sum_{j=1}^{F}(Y_{ij} - \bar{Y})^2}} \tag{5}$$

The CMC quantifies reliability between sessions, with values approaching 1 indicating waveform overlap after compensating for systematic biases.

2.3.5. Cognitive Metrics

To quantify the cognitive demands of the dual-task conditions, we analyzed pupil diameter data continuously recorded by the integrated eye-tracking system. Raw bilateral pupil signals were preprocessed by detecting and removing blink artifacts, applying linear interpolation to fill the resulting data gaps, and averaging the left and right pupil diameters to obtain a unified continuous time series. Cognitive effort was then evaluated using two complementary indices: normalized continuous pupil dilation and the Task-Evoked Pupillary Response (TEPR).

First, to assess sustained cognitive workload, we analyzed the continuous pupil dilation. In cognitive pupillometry, the continuous (or tonic) pupil diameter serves as a reliable physiological proxy for autonomic nervous system arousal, reflecting the sustained mental effort required to engage in a prolonged activity [30,31]. To account for inherent inter-subject variability in resting pupil size, these raw measurements were z-score normalized for each participant across all experimental conditions.

Second, to capture the acute mental effort associated with processing individual stimuli, we calculated the Task-Evoked Pupillary Response (TEPR) [32,33]. This metric evaluates the phasic pupillary dilation triggered by a specific cognitive event, in our case the cognitive task of identifying the target stimulus. The TEPR was extracted by time-locking the preprocessed pupil signal to the exact onset of each target green number (t=0). A pre-stimulus baseline ($D_{baseline}$) was established using the mean pupil diameter over a 1-second window immediately preceding the stimulus appearance (from $t = -1$ s to $t = 0$ s). Subsequently, the peak pupil diameter (D_{max}) was identified within a 2-second post-stimulus window (from $t = 0$ s to $t = 2$ s). The TEPR was then computed as the maximum proportional increase relative to the baseline, expressed through the following equation:

$$TEPR = \frac{D_{max} - D_{baseline}}{D_{baseline}} \tag{6}$$

By isolating this phasic response, this metric quantifies the immediate cognitive cost of identifying and processing the target, independently of the user's overall tonic arousal.

 doi:10.20944/preprints202604.0925.v1

2.4. Experimental Setup

The experimental protocol included sessions with the exoskeleton alone (training), the VR headset alone (single-task test), and a combination of both (dual-task test). To simulate a realistic walking scenario, all experiments were conducted in a standard corridor under ecological conditions, relying only on the building's standard artificial illumination without any special brightness control equipment. Data acquisition across all sensors and the Meta Quest 3 application was triggered simultaneously via a custom Python-based program. Specifically, this program executed shell commands via TCP/IP protocols and proprietary libraries to remotely initiate the Unity application on the Meta Quest and start the eye-tracking recording on the Pupil Neon hardware. Concurrently, the interface triggered the Xsens motion capture recording locally on the host PC. All devices were connected to the same local network to establish a shared temporal reference, and the synchronization between the Meta Quest and Pupil eye-tracking data streams was subsequently fine-tuned offline using cross-correlation and mathematical optimization.

2.5. Experimental Protocol

To validate the protocol, 30 healthy subjects (15 male and 15 females) have voluntarily participated in the experiment following the protocol in Figure 3. The recruited participants were aged between 20 and 40 years old, ranging in height from 160 to 185 cm, with a body weight not exceeding 80 kg. The study was performed according to the guidelines of the Ethics Committee for University Research of the University of Brescia, identified with the code 45/2025.

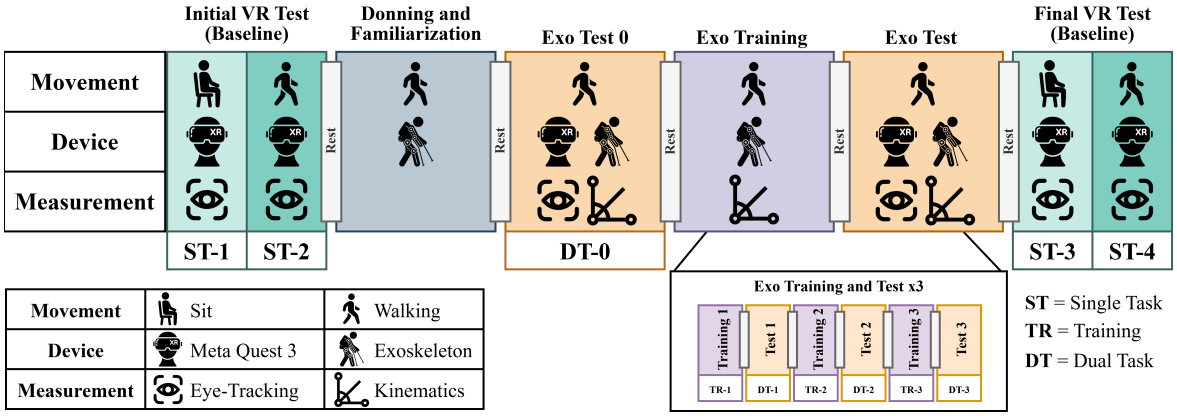

Figure 3. Schematic overview of the experimental protocol. The timeline illustrates the sequence of Single Task (ST) and Dual Task (DT) conditions. The protocol begins with initial XR assessments (ST-1, ST-2), followed by exoskeleton donning and a baseline dual-task test (DT-0). Participants then undergo three consecutive cycles of exoskeleton training (TR-1 to TR-3) and dual-task testing (DT-1 to DT-3), concluding with final XR assessments (ST-3, ST-4). The grid explicitly details the movements (sitting, walking), involved devices (Meta Quest 3, Exoskeleton), and the acquired data (Eye-Tracking, Kinematics) for each corresponding phase. Interleaved "Rest" blocks denote pauses between tasks.

The experimental protocol begins with an Initial VR Test (Baseline). For each trial involving the headset, the task concluded once the subject was presented with 20 numbers within the application, resulting in a duration of approximately 2.5 minutes per session. During this initial baseline phase, the subject wears a Meta Quest 3 headset and performs tasks in both a seated (ST-1) and walking (ST-2) position. Through the headset, only Eye-Tracking data is recorded to establish an attentional baseline. To mitigate the effects of physical and cognitive fatigue, custom-duration rest periods are integrated between all consecutive testing and training phases.

Then, a 15-minute session is dedicated to donning the exoskeleton, and a brief familiarization with the exoskeleton is performed to adjust the device's parameters to the individual's biomechanical needs.

 doi:10.20944/preprints202604.0925.v1

Following this adaptation and an additional rest period, Exo Test 0 (DT-0) is conducted. The participant walks while simultaneously wearing the exoskeleton and the Meta Quest 3. During this initial stage of combined use, both Kinematics and Eye-Tracking data are acquired simultaneously.

After this initial measurement, the protocol employs an iterative loop to evaluate the progression of the user's motor adaptation. This loop consists of an Exo Training session (TR), where the subject walks with only the exoskeleton while kinematic data is recorded, followed by an Exo Test (DT) phase. The Exo Test replicates the exact conditions of Exo Test 0, acquiring both kinematic and ocular data while the subject walks with the exoskeleton and interacts with the Meta Quest 3. As detailed in the diagram (Exo Training and Test x3), this combined block is repeated three consecutive times in an alternating fashion, with rest periods interspersed between each individual training and test session to capture progressive adaptation.

Finally, the protocol concludes with a Final VR Test (Baseline). Mirroring the initial phase, the participant performs seated and walking tasks wearing only the Meta Quest 3 headset (monitored via eye-tracking). This procedure is designed to capture concluding cognitive metrics and account for any potential fatigue accumulated throughout the entire experiment.

2.6. Statistical Analysis

Prior to the main statistical analyses, the Lilliefors test was conducted to evaluate the normality of the data distributions.

For the kinematic parameters (SLV, SPARC and CMC), the null hypothesis of normality was not rejected in any of the experimental conditions, justifying the use of parametric statistics. Accordingly, Linear Mixed Models (LMMs) were implemented. The LMMs included the experimental *Session* and the *Task* modality (Training vs. Dual Task) as interacting fixed effects, while the *Subject* was modeled as a random intercept to account for individual baseline differences (model formulation: `Metric ~ Session * Task + (1|Subject)`).

To specifically assess how training impacted performance under cognitive load, we targeted our analysis on the dual-task conditions. Accordingly, an omnibus Analysis of Variance (ANOVA) was performed on the Dual Task conditions. For any significant effects, subsequent post-hoc pairwise comparisons were conducted to assess adaptation further.

For the cognitive workload analysis based on pupillometry, the Lilliefors test revealed that not all conditions met the assumption of normality. Consequently, a non-parametric statistical approach was adopted. Global differences in the normalized continuous pupil dilation across the experimental conditions were evaluated using the Friedman test. When significant main effects were detected, post-hoc pairwise comparisons were conducted using the Wilcoxon signed-rank test to identify specific condition-level differences.

Finally, to mathematically model the cognitive adaptation over time, LMMs were fitted for the Task-Evoked Pupillary Response (TEPR) isolated during the exoskeleton-assisted sessions. In these specific models, the longitudinal *Session* was treated as a fixed effect to capture the time-dependent learning trend, with the *Subject* included as a random intercept (model formulation: `Metric ~ Session + (1|Subject)`).

3. Results

3.1. Kinematics Results

Table 1 details the statistical evaluation of the three extracted kinematic metrics, summarizing the outcomes of both the LMMs and the subsequent post-hoc comparisons across the Dual Task conditions.

The LMM analysis of the Step Length Variability (SLV) (Figure 4) indicated no significant baseline difference between the conditions ($p = 0.085$). A highly significant main effect of Session was found ($p < 0.001$), demonstrating a decrease in gait variability over time. Furthermore, a significant Session × Task interaction was detected ($p = 0.020$), indicating that the reduction in variability observed in the Dual Task condition was absent in the Training condition. Post-hoc comparisons on Dual-Task sessions

 doi:10.20944/preprints202604.0925.v1

indicated that the initial assessment DT-0 was characterized by significantly higher spatial variability compared to condition DT-1 (p = 0.006) and condition DT-3 (p = 0.007), although the difference with condition DT-2 did not reach statistical significance (p = 0.107). No significant differences were observed among the subsequent assessments (DT-1, DT-2, and DT-3).

Table 1. Summary of the statistical analysis including Linear Mixed-Effects Models (LMM) for longitudinal predictive trends and Repeated Measures ANOVA for condition-based motor adaptation.

Statistical Test	Effect / Comparison	Test Statistic	p-value
	Step Length Variability		
LMM	Main Effect: Session	$\beta = -0.586$	< 0.001
LMM	Interaction: Session × Task	$\beta = 0.626$	0.020
RM-ANOVA	Main Effect: Condition	$\eta_p^2 = 0.267$	< 0.001
Post-Hoc (Bonferroni)	DT-0 vs. DT-1	$d = 0.711$	0.006
Post-Hoc (Bonferroni)	DT-0 vs. DT-3	$d = 0.701$	0.007
Post-Hoc (Bonferroni)	DT-1 vs. DT-2	-	0.295 (ns)
	SPARC V_SHANK		
LMM	Main Effect: Session	$\beta = 0.013$	< 0.001
LMM	Interaction: Session × Task	$\beta = -0.015$	0.019
RM-ANOVA	Main Effect: Condition	$\eta_p^2 = 0.225$	< 0.001
Post-Hoc (Bonferroni)	DT-0 vs. DT-1	$d = 0.812$	0.002
Post-Hoc (Bonferroni)	DT-0 vs. DT-3	$d = 0.582$	0.033
Post-Hoc (Bonferroni)	DT-1 vs. DT-2	-	1.000 (ns)
	CMC V_SHANK		
LMM	Main Effect: Session	$\beta = 0.007$	< 0.001
LMM	Interaction: Session × Task	$\beta = -0.004$	0.073 (ns)
RM-ANOVA	Main Effect: Condition	$\eta_p^2 = 0.439$	< 0.001
Post-Hoc (Bonferroni)	DT-0 vs. DT-1	$d = 1.093$	< 0.001
Post-Hoc (Bonferroni)	DT-0 vs. DT-3	$d = 1.014$	< 0.001
Post-Hoc (Bonferroni)	DT-1 vs. DT-2	-	1.000 (ns)

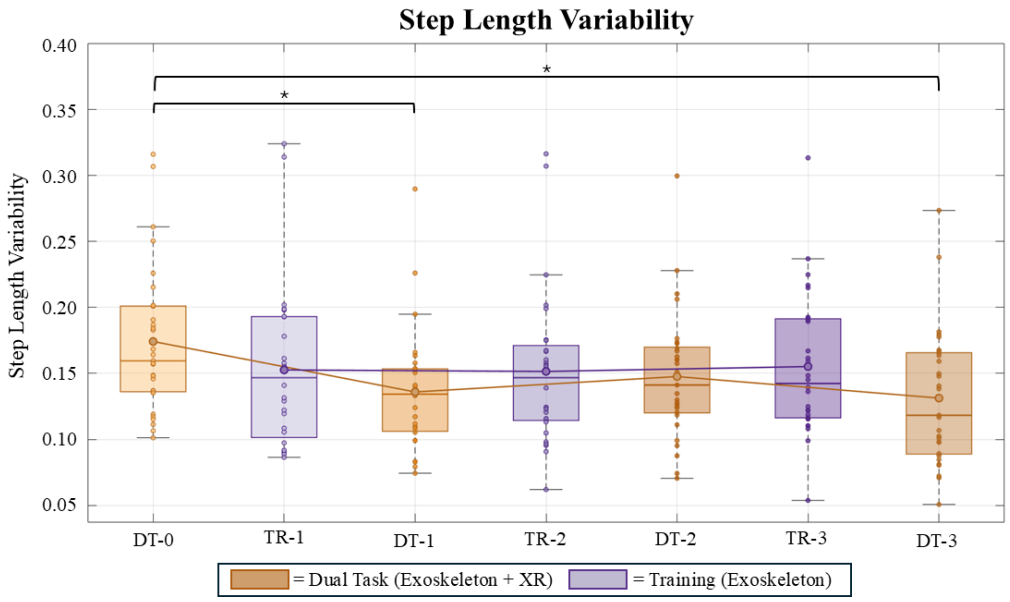

Figure 4. Step Length Variability (SLV) across the sequence of training (TR) and dual-task (DT) assessment sessions. Orange boxes denote the Dual-Task condition (Exoskeleton + XR Headset), and purple boxes denote the Training condition (Exoskeleton only). Solid lines connect the mean values across conditions. Statistically significant differences between sessions are indicated by black brackets with asterisks (* p < 0.05).

 doi:10.20944/preprints202604.0925.v1

The LMM analysis of the Spectral Arc Length (SPARC, Figure 5), where less negative values indicate a smoother gait, the model revealed a significant main effect of Task at baseline ($p = 0.023$), confirming that subjects initially exhibited a significantly smoother movement during the Training. A significant main effect of Session was also observed ($p < 0.001$), showing a clear improvement in smoothness over time during the Dual Task condition. Crucially, a significant Session × Task interaction was found ($p = 0.019$), demonstrating that while smoothness significantly improved over the sessions in the Dual Task, it remained relatively stable in the ST, leading to a progressive convergence of the two conditions. Post-hoc comparison on Dual-Task sessions revealed that movement smoothness was significantly lower at condition DT-0 compared to condition DT-1 ($p = 0.002$), condition DT-2 ($p = 0.037$), and condition DT-3 ($p = 0.033$). No significant differences were observed among the subsequent assessments (DT-1, DT-2, and DT-3).

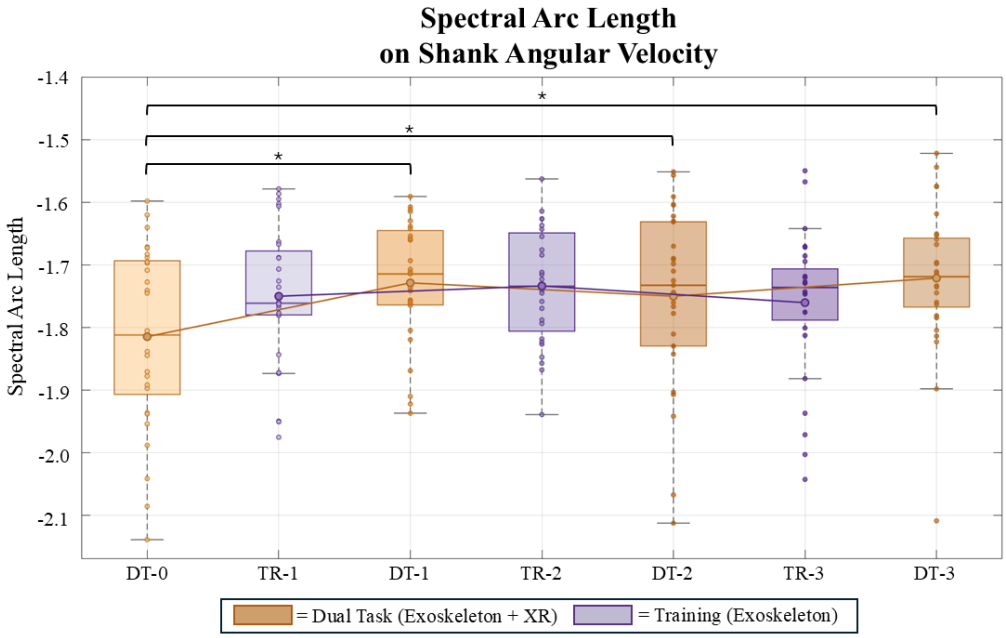

Figure 5. Spectral Arc Length (SPARC) on the Shank Angular Velocity across the sequence of training (TR) and dual-task (DT) assessment sessions. Orange boxes denote the Dual-Task condition (Exoskeleton + XR Headset), and purple boxes denote the Training condition (Exoskeleton only). Solid lines connect the mean values across conditions. Statistically significant differences between sessions are indicated by black brackets with asterisks (* $p < 0.05$).

The LMM analysis on the Coefficient of Multiple Correlation (CMC, Figure 6) of the shank angular velocity demonstrated a highly significant positive main effect of Session ($p < 0.001$), indicating that movement similarity significantly improved over time. The baseline difference between the Training and Dual Task was not statistically significant ($p = 0.147$), and the Session × Task interaction only showed a trend without reaching statistical significance ($p = 0.073$), suggesting that the rate of improvement was not structurally different between the two conditions. Post-hoc analysis demonstrated that the initial consistency in condition DT-0 was significantly lower than in all subsequent Dual-Task sessions ($p < 0.001$ for all comparisons against conditions DT-1, DT-2 and DT-3). Consistent with the other results, the CMC values plateaued after the initial assessment, with no significant differences found between conditions DT-1, DT-2, and DT-3 (all $p > 0.05$).

Taken together, these intra-condition analyzes clarify the LMM findings by confirming a nonlinear adaptation process during the Dual Task, where the most substantial biomechanical improvements in stability, consistency, and smoothness occur abruptly after the first evaluation, followed by a plateau in the subsequent phases.

 doi:10.20944/preprints202604.0925.v1

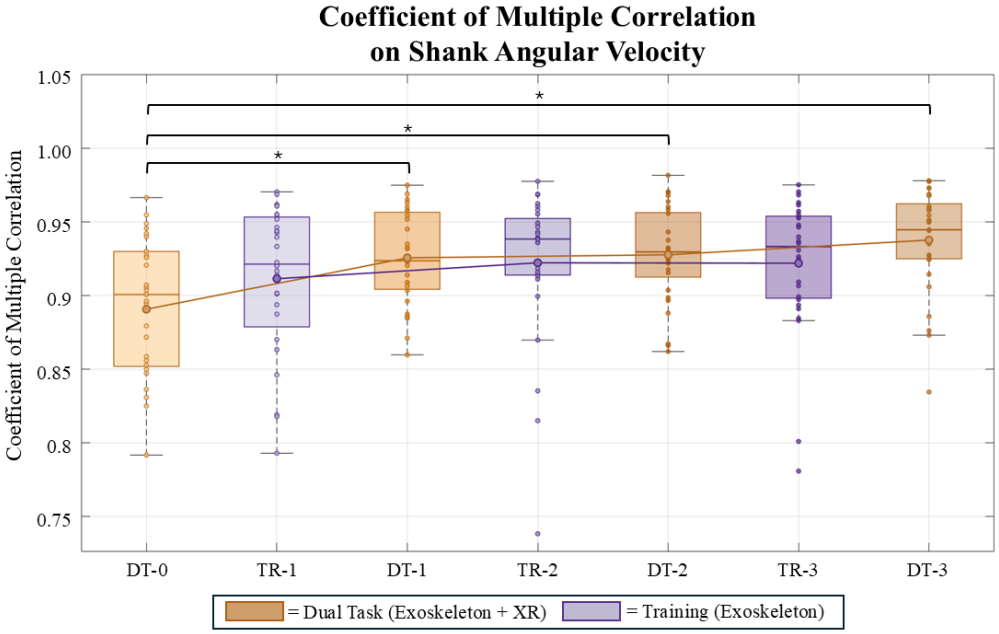

Figure 6. Coefficient of Multiple Correlation (CMC) on the Shank Angular Velocity across the sequence of training (TR) and dual-task (DT) assessment sessions. Orange boxes denote the Dual-Task condition (Exoskeleton + XR Headset), and purple boxes denote the Training condition (Exoskeleton only). Solid lines connect the mean values across conditions. Statistically significant differences between sessions are indicated by black brackets with asterisks (* $p < 0.05$).

3.1.1. Cognitive Results

Table 2 summarizes the statistical outcomes for the two evaluated cognitive metrics: normalized continuous pupil dilation and the Task-Evoked Pupillary Response (TEPR). Differences in continuous pupil dilation across the experimental conditions were analyzed using a non-parametric Friedman test, followed by Wilcoxon signed-rank tests for post-hoc pairwise comparisons. Conversely, the TEPR during the exoskeleton-assisted Dual-Task sessions was analyzed by fitting Linear Mixed-Effects Models (LMM).

Table 2. Summary of the statistical analysis including the Linear Mixed Model (LMM) for the Task-Evoked Pupillary Response (TEPR) learning trend and the Friedman test for condition-based pupil dilation adaptation.

Statistical Test	Effect / Comparison	Test Statistic	p-value
Pupil Dilation (z-score normalized)			
Friedman Test	Main Effect: Condition	$W = 0.431$	< 0.001
Post-Hoc (Wilcoxon)	ST-1 vs. DT-0	$r = 0.803$	< 0.001
Post-Hoc (Wilcoxon)	ST-1 vs. ST-2	$r = 0.498$	0.0215
Post-Hoc (Wilcoxon)	All DT cond. (pairwise)	-	$0.681 < p < 0.927$ (ns)
Post-Hoc (Wilcoxon)	ST-1 vs. ST-3	-	0.1023 (ns)
Task-Evoked Pupillary Response (TEPR)			
LMM	Main Effect: Session	$\beta = -0.0058$	0.025

The Z-score normalized pupil dilation was analyzed across eight experimental phases, comprising four Single Task (ST-1 to ST-4) and four Dual Task (DT-1 to DT-4) conditions. A non-parametric Friedman test revealed a significant main effect of the experimental condition on pupil dilation ($p < 0.001$). Post-hoc pairwise comparisons using the Wilcoxon signed-rank test showed that normalized pupil dilation during all DT phases was significantly higher compared to the ST phases ($p < 0.001$ for most comparisons). No significant differences were found when comparing the four DT blocks with each other (p-values ranging from 0.681 to 0.927). Conversely, statistically significant variations were observed within the Single Task conditions, specifically between ST-1 and ST-2 ($p = 0.0215$) and

 doi:10.20944/preprints202604.0925.v1

between ST-3 and ST-4 ($p = 0.0342$), which correspond to the seated (ST-1, ST-3) and walking (ST-2, ST-4) task modalities.

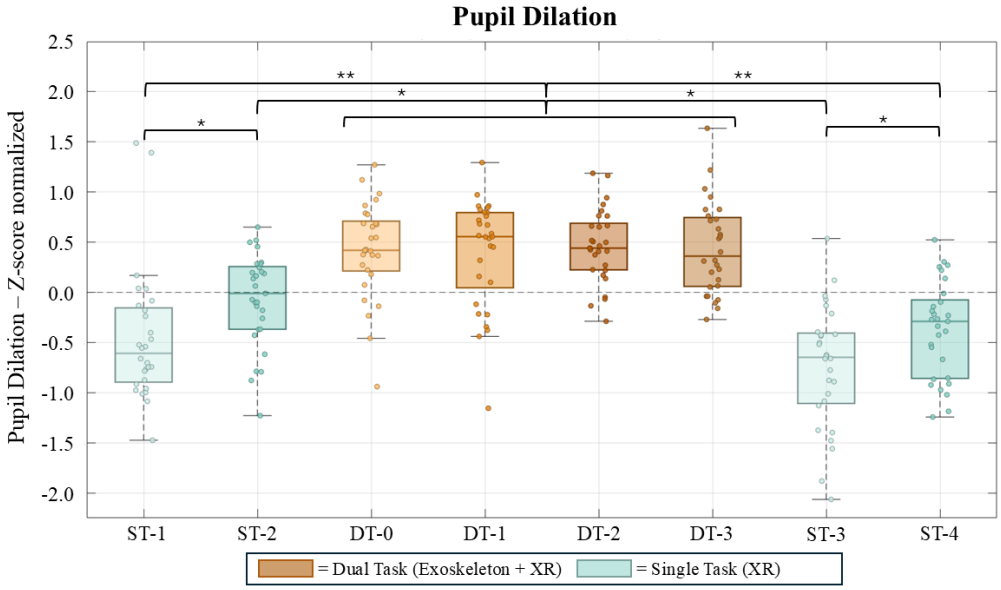

Figure 7. Z-score normalized pupil dilation across Single Task (ST, light blue) and Dual Task (DT, orange) experimental conditions. Statistically significant differences between sessions are indicated by black brackets with asterisks (p<0.05 * and p<0.001 **).

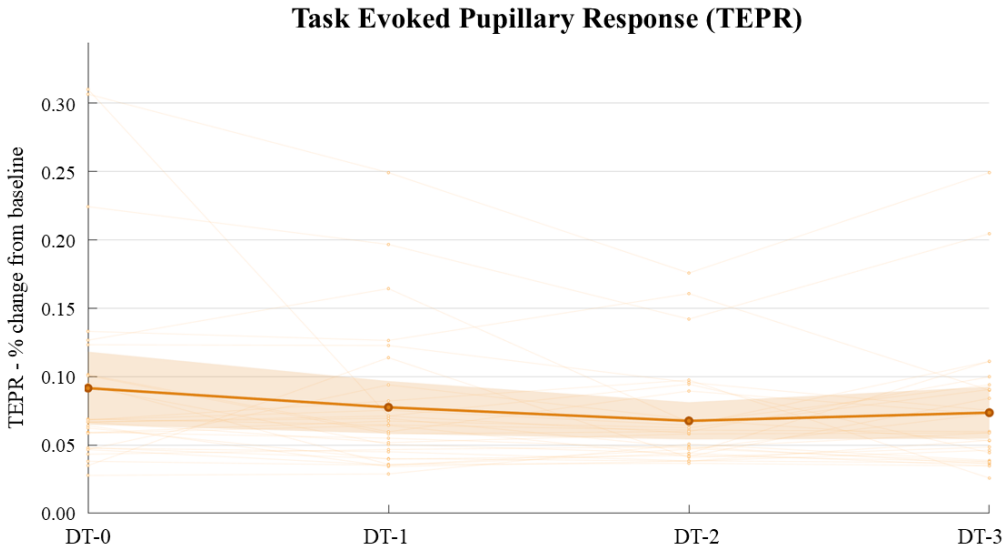

Figure 8. Task-Evoked Pupillary Response (TEPR), expressed as the percentage change from baseline, across the four consecutive DT sessions. Thin faded lines illustrate individual participant trends, while the bold solid line represents the group mean alongside its shaded confidence interval.

The Task-Evoked Pupillary Response (TEPR), expressed as the percentage change from baseline, was analyzed across the four repeated Dual Task (DT) sessions. A Linear Mixed Model (LMM) was employed to assess the fixed effect of the 'Session', accounting for inter-subject variability. The LMM analysis revealed a statistically significant, small negative effect of the session progression on the TEPR amplitude ($\beta = -0.0058$, $p = 0.0255$), with an estimated intercept of 0.0928 ($p < 0.001$), representing an initial average TEPR of approximately 9.28% above baseline.

Ultimately, these results demonstrate that while the overall tonic dilation remained consistently high during complex tasks, the amplitude of the phasic pupillary response decreased linearly, suggesting a subtle adaptation to the Dual Task over time.

 doi:10.20944/preprints202604.0925.v1

4. Discussions

The primary objective of this study was to validate a protocol for quantifying motor and cognitive adaptation during human-exoskeleton interaction. Before deploying such a complex architecture in clinical populations, it was essential to verify its reliability on a controlled cohort. The findings confirm the robustness of the proposed protocol. The integrated system successfully captured the dynamics of dual-task interference, tracking the transition from initial motor disruption to the eventual motor learning and stabilization.

4.1. Kinematics

Initially, the Linear Mixed-Effects Models (LMM) revealed a clear pattern of cognitive-motor interference. After the brief initial familiarization with the exoskeleton, when the concurrent cognitive task was introduced, the micro-control of movement was disrupted, resulting in lower movement smoothness (SPARC) and higher Step Length Variability. This aligns with the capacity-sharing theory: dividing attention between a motor and a cognitive task compromises the online feedback control of gait. Interestingly, the macro-structure of the gait pattern, measured by kinematic consistency (CMC), was less impacted at baseline. This is likely because fundamental rhythmic locomotion is governed by lower-level Central Pattern Generators (CPGs), which are highly resilient to cognitive distraction [34], [35]. Crucially, our measurement architecture captured a counterintuitive trend: as subjects automated the cognitive demands, the Dual Task (DT) performances did not just recover but eventually surpassed the Training (TR) baseline. By the end of the protocol, the architecture quantified smoother movements, higher consistency, and lower variability in the Dual Task condition compared to the Training. From a metrological standpoint, the ability to track this continuous functional improvement—without instrumental drift over multiple sessions—strongly validates the robustness of the selected metrics.

Furthermore, the intra-condition analysis (Repeated Measures ANOVA) on the longitudinal DT assessments highlighted the system's accuracy in measuring the actual physical constraints of robotic assistance. The data revealed a non-linear motor adaptation: the most substantial biomechanical improvements occurred abruptly between the first and second Dual Task assessments (DT-1, DT-2), immediately followed by a statistically robust plateau. This rapid stabilization is both biologically and mechanically sound. First, the healthy participants in this study possess intact neural circuitry and high cognitive reserve, which enable extremely fast motor learning when facing new dual-task challenges. Second, and most importantly, the active exoskeleton inherently restricts the user's movements by imposing predefined spatial trajectories and fixed assistance timings. The initial drop in performance simply reflects a brief user-robot desynchronization caused by cognitive distraction. Once the subjects learned to "trust" the exoskeleton and stopped consciously fighting its assistance, they synchronized with the robot's rhythm. Because the device fundamentally dictates the joint kinematics, the performance metrics quickly reached a mechanical ceiling (for CMC and SPARC) and a floor (for variability). The fact that our sensing architecture accurately recorded this plateau, without showing random noise or artifactual fluctuations in the later sessions, confirms its high reliability. It effectively measures the true physical boundaries imposed by the exoskeleton, proving to be a valid and ready-to-use tool for future clinical applications involving neurologically impaired patients.

4.2. Cognitive

The cognitive assessment via pupillometry provided insights into how users allocate mental resources during exoskeleton-assisted overground walking. The continuous (tonic) pupil dilation, a physiological proxy for sustained arousal and general mental effort [32], was significantly elevated during all Dual Task (DT) phases compared to Single Task (ST) conditions. This physiological distinction highlights the cognitive overhead required to coordinate robotic assistance while simultaneously scanning the peripheral environment. Notably, the tonic dilation remained consistently high and stable across the four DT blocks. This lack of habituation in baseline arousal aligns with existing literature on cognitive-motor interference, which suggests that dynamic postural control and locomo-

 doi:10.20944/preprints202604.0925.v1

tion—especially when using an external assistive device—demand continuous executive functioning that does not rapidly automate in novice users [36,37].

In contrast, the Task-Evoked Pupillary Response (TEPR) successfully captured the acute, phasic mental effort strictly associated with processing the target stimuli. While the initial TEPR amplitude indicated a high immediate cognitive cost (averaging a 9.28% increase above baseline), the Linear Mixed-Effects Model revealed a significant, progressive decrease in this phasic response across the sessions. This gradual reduction in TEPR amplitude points toward a specific cognitive adaptation or learning effect related to the visual search task itself. As users became more familiar with the spatial layout of the holographic grid and the color-coded targets, their perceptual processing became more efficient, demanding fewer acute cognitive resources per stimulus [32].

These cognitive findings serve as a validation of our measurement protocol. The integrated system successfully separated two distinct mental processes occurring at the same time. On one hand, the continuous pupil dilation remained stable, reflecting the constant effort required to walk safely with the exoskeleton. On the other hand, the TEPR progressively decreased, showing that users were learning and adapting to the visual game.

Combining kinematic and cognitive data explains how users handle dual-task interference. The results suggest that motor performance and mental load linked over time. The first dual-task block (DT-0) is the most challenging. In this phase, acute cognitive demand (TEPR) reaches its peak. At the same time, walking results unstable. Step variability increases, and movement smoothness drops. However, gait stabilizes rapidly in the following blocks (DT-1 to DT-3). During this motor recovery, sustained mental effort (continuous pupil dilation) stays consistently high. On the other hand, the acute cost of the visual task (TEPR) steadily decreases. This specific pattern points to a 'posture-first' strategy [36]. Users constantly dedicate high mental resources to walk safely with the exoskeleton. Meanwhile, they quickly adapt to the visual game. This habituation frees up acute cognitive resources. As a result, users can quickly restore and maintain their walking stability.

5. Conclusions

This study successfully validated a novel sensing framework designed to monitor human-exoskeleton interaction. The system captured the initial cognitive-motor interference, marked by disrupted gait control and sustained pupil dilation. It also successfully tracked the subsequent non-linear motor learning trend. Specifically, the framework detected a mechanical performance plateau imposed by the exoskeleton. At the same time, it recorded the physiological adaptation, highlighted by TEPR attenuation, that explains the eventual 'overshoot' of baseline motor performance. Together, these findings confirm the reliability of the proposed architecture for continuous, ecological monitoring.

Despite these promising findings, certain limitations must be acknowledged. First, the relatively small sample size restricts the broader generalizability of the statistical results. Second, the protocol was tested exclusively on healthy individuals. These participants do not fully reflect the clinical target demographic, such as stroke or spinal cord injury survivors. Third, the system was validated using a single commercial exoskeleton model. Different robotic devices employ distinct control algorithms and assistance levels. Consequently, the current protocol may require adjustments before serving as a standard across diverse assistive platforms.

Building on these findings, future research will expand in several key directions. First, we will investigate the rapid early adaptation phase with higher temporal resolution by segmenting the initial dual-task block into smaller analytical epochs. Second, we aim to identify subject-specific learning strategies by exploring behavioral clusters within the cohort. Third, the analytical framework will be enriched with additional eye-tracking metrics, such as fixation durations and behavioral reaction times, to establish direct statistical correlations between kinematic improvements and cognitive engagement. Finally, a dedicated longitudinal study will isolate the exoskeleton learning curve, comparing purely motor training (Single Task) against concurrent training (Dual Task). This will thoroughly test the

 doi:10.20944/preprints202604.0925.v1

hypothesis that introducing a cognitive challenge, despite causing lower initial performance, may actually accelerate motor learning and ultimately produce a superior gait pattern.

Author Contributions: Conceptualization, N.A., E.S., D.T. and M.L.; methodology, N.A., M.L., D.T.; software, N.A. and R.C.; validation, N.A.; formal analysis, N.A. and R.C.; investigation, N.A. and R.C; resources, D.T. and M.L.; data curation, N.A.; writing—original draft preparation, N.A.; writing—review and editing, E.S., D.T. and M.L; visualization, N.A. and M.L.; supervision, M.L. and D.T.; project administration, M.L.; funding acquisition, M.L. All authors have read and agreed to the published version of the manuscript.

Funding: Funded by the European Union-NextGeneration EU, Mission 4 Component 1 CUP D82B23003070001

Institutional Review Board Statement: The study was conducted in accordance with the Declaration of Helsinki, and approved by the Ethics Committee for University Research of the University of Brescia (45/2025, 24/11/2025)

Informed Consent Statement: Written informed consent has been obtained from the volunteers to publish this paper

Data Availability Statement: The data presented in this study are available on request from the corresponding author. The data are not publicly available due to privacy and ethical restrictions regarding human subjects, as mandated by the Ethics Committee for University Research of the University of Brescia. All data are stored anonymized in a dedicated secure database.

Acknowledgments: The authors would like to express their gratitude to Technaid for providing the Exo-H3 exoskeleton and for their valuable technical support throughout the experimental phase. During the preparation of this manuscript, the author(s) used Gemini Pro for the purpose of rephrasing sentences. The authors have reviewed and edited the output and take full responsibility for the content of this publication

Conflicts of Interest: The authors declare no conflicts of interest.

References

1. Rupal, B.S.; Rafique, S.; Singla, A.; Singla, E.; Isaksson, M.; Virk, G.S. Lower-limb exoskeletons: Research trends and regulatory guidelines in medical and non-medical applications. *International Journal of Advanced Robotic Systems* **2017**, *14*, 1729881417743554. https://doi.org/10.1177/1729881417743554.
2. Pinto-Fernandez, D.; Torricelli, D.; Sanchez-Villamanan, M.d.C.; Aller, F.; Mombaur, K.; Conti, R.; Vitiello, N.; Moreno, J.C.; Pons, J.L. Performance Evaluation of Lower Limb Exoskeletons: A Systematic Review. *IEEE Transactions on Neural Systems and Rehabilitation Engineering* **2020**, *28*, 1573–1583. https://doi.org/10.1109/TNSRE.2020.2989481.
3. Young, A.J.; Ferris, D.P. State of the Art and Future Directions for Lower Limb Robotic Exoskeletons. *IEEE transactions on neural systems and rehabilitation engineering: a publication of the IEEE Engineering in Medicine and Biology Society* **2017**, *25*, 171–182. https://doi.org/10.1109/TNSRE.2016.2521160.
4. Wilkenfeld, J.N.; Kim, S.; Upasani, S.; Kirkwood, G.L.; Dunbar, N.E.; Srinivasan, D. Sensemaking, adaptation and agency in human-exoskeleton synchrony. *Frontiers in Robotics and AI* **2023**, *10*. https://doi.org/10.3389/frobt.2023.1207052.
5. Marchand, C.; De Graaf, J.B.; Jarrassé, N. Measuring mental workload in assistive wearable devices: a review. *Journal of NeuroEngineering and Rehabilitation* **2021**, *18*, 160. https://doi.org/10.1186/s12984-021-00953-w.
6. Charles, R.L.; Nixon, J. Measuring mental workload using physiological measures: A systematic review. *Applied Ergonomics* **2019**, *74*, 221–232. https://doi.org/10.1016/j.apergo.2018.08.028.
7. Heller, B.W.; Datta, D.; Howitt, J. A pilot study comparing the cognitive demand of walking for transfemoral amputees using the Intelligent Prosthesis with that using conventionally damped knees. *Clinical Rehabilitation* **2000**, *14*, 518–522. https://doi.org/10.1191/0269215500cr345oa.
8. Miller, W.C.; Speechley, M.; Deathe, B. The prevalence and risk factors of falling and fear of falling among lower extremity amputees. *Archives of Physical Medicine and Rehabilitation* **2001**, *82*, 1031–1037. https://doi.org/10.1053/apmr.2001.24295.
9. Yuan, J.; Bai, X.; Driscoll, B.; Liu, M.; Huang, H.; Feng, J. Standing and Walking Attention Visual Field (SWAVF) task: A new method to assess visuospatial attention during walking. *Applied Ergonomics* **2022**, *104*, 103804. https://doi.org/10.1016/j.apergo.2022.103804.

 doi:10.20944/preprints202604.0925.v1

10. Althomali, M.M.; Leat, S.J. Binocular Vision Disorders and Visual Attention: Associations With Balance and Mobility in Older Adults. *Journal of Aging and Physical Activity* **2018**, *26*, 235–247. https://doi.org/10.1123/japa.2016-0349.
11. Mirelman, A.; Herman, T.; Brozgol, M.; Dorfman, M.; Sprecher, E.; Schweiger, A.; Giladi, N.; Hausdorff, J.M. Executive Function and Falls in Older Adults: New Findings from a Five-Year Prospective Study Link Fall Risk to Cognition. *PLoS ONE* **2012**, *7*, e40297. https://doi.org/10.1371/journal.pone.0040297.
12. Lim, J.; Amado, A.; Sheehan, L.; Van Emmerik, R.E.A. Dual task interference during walking: The effects of texting on situational awareness and gait stability. *Gait & Posture* **2015**, *42*, 466–471. https://doi.org/10.1016/j.gaitpost.2015.07.060.
13. Simons, D.J.; Chabris, C.F. Gorillas in our midst: sustained inattentional blindness for dynamic events. *Perception* **1999**, *28*, 1059–1074. https://doi.org/10.1068/p281059.
14. Parr, J.V.V.; Vine, S.J.; Wilson, M.R.; Harrison, N.R.; Wood, G. Visual attention, EEG alpha power and T7-Fz connectivity are implicated in prosthetic hand control and can be optimized through gaze training. *Journal of Neuroengineering and Rehabilitation* **2019**, *16*, 52. https://doi.org/10.1186/s12984-019-0524-x.
15. Upasani, S.; Srinivasan, D. Gaze Behavior and Mental Workload While Using a Whole-Body Powered Exoskeleton: A Pilot Study. *Proceedings of the Human Factors and Ergonomics Society Annual Meeting* **2023**, *67*, 980–981. https://doi.org/10.1177/21695067231192201.
16. Mariani, G.; Lambranzi, C.; Cartocci, N.; Barresi, G.; Natali, C.D.; Momi, E.D.; Ortiz, J. Physiological Measures of the Mental Workload in Users of a Lower Limb Exosuit: A Comparison of Subjective and Objective Metrics, 2025. arXiv:2511.11414 [eess], https://doi.org/10.48550/arXiv.2511.11414.
17. Leibman, D.; Mitchell, D.B.; Choi, H. Impacts of Enhanced Physical Abilities via Exoskeletons on Attentional Performance and Workload - Daniel Leibman, Daxton B. Mitchell, HeeSun Choi, 2022. *Proceedings of the Human Factors and Ergonomics Society Annual Meeting* **2022**.
18. Leibman, D.; Choi, H. Changes in the Distribution of Visual Attention Associated with Lower-Body and Back-Support Exoskeleton Use During Lifting Task - Daniel Leibman, HeeSun Choi, 2025. *Proceedings of the Human Factors and Ergonomics Society Annual Meeting* **2025**.
19. Ayed, I.; Ghazel, A.; Jaume-I-Capó, A.; Moyà-Alcover, G.; Varona, J.; Martínez-Bueso, P. Vision-based serious games and virtual reality systems for motor rehabilitation: A review geared toward a research methodology. *International Journal of Medical Informatics* **2019**, *131*, 103909. https://doi.org/10.1016/j.ijmedinf.2019.06.016.
20. Rodrigues-Carvalho, C.; Fernández-García, M.; Pinto-Fernández, D.; Sanz-Morere, C.; Barroso, F.O.; Borromeo, S.; Rodríguez-Sánchez, C.; Moreno, J.C.; del Ama, A.J. Benchmarking the Effects on Human–Exoskeleton Interaction of Trajectory, Admittance and EMG-Triggered Exoskeleton Movement Control. *Sensors* **2023**, *23*. https://doi.org/10.3390/s23020791.
21. Massardi, S.; Rodriguez-Cianca, D.; Pinto-Fernandez, D.; Moreno, J.C.; Lancini, M.; Torricelli, D. Characterization and Evaluation of Human–Exoskeleton Interaction Dynamics: A Review. *Sensors* **2022**, *22*. https://doi.org/10.3390/s22113993.
22. Smit-Russcher, R.; Princelle, D.; Bilal, I. MVN white paper: Enhancing motion tracking accuracy with novel gender-specific models.
23. Grimmer, M.; Schmidt, K.; Duarte, J.E.; Neuner, L.; Koginov, G.; Riener, R. Stance and Swing Detection Based on the Angular Velocity of Lower Limb Segments During Walking. *Frontiers in Neurorobotics* **2019**, *13*. https://doi.org/10.3389/fnbot.2019.00057.
24. Montero-Odasso, M.; Muir, S.W.; Speechley, M. Dual-task complexity affects gait in people with mild cognitive impairment: the interplay between gait variability, dual tasking, and risk of falls. *Archives of Physical Medicine and Rehabilitation* **2012**, *93*, 293–299. https://doi.org/10.1016/j.apmr.2011.08.026.
25. Demirdel, S.; Erbahçeci, F.; Yazıcıoğlu, G. The effects of cognitive versus motor concurrent task on gait in individuals with transtibial amputation, transfemoral amputation and in a healthy control group. *Gait & Posture* **2022**, *91*, 223–228. https://doi.org/10.1016/j.gaitpost.2021.10.036.
26. Rock, C.G.; Marmelat, V.; Yentes, J.M.; Siu, K.C.; Takahashi, K.Z. Interaction between step-to-step variability and metabolic cost of transport during human walking. *The Journal of Experimental Biology* **2018**, *221*, jeb181834. https://doi.org/10.1242/jeb.181834.
27. Beck, Y.; Herman, T.; Brozgol, M.; Giladi, N.; Mirelman, A.; Hausdorff, J.M. SPARC: a new approach to quantifying gait smoothness in patients with Parkinson's disease. *Journal of Neuroengineering and Rehabilitation* **2018**, *15*, 49. https://doi.org/10.1186/s12984-018-0398-3.
28. Antonelli, M.; Caselli, E.; Gastaldi, L. Comparison of Gait Smoothness Metrics in Healthy Elderly and Young People. *Applied Sciences* **2024**, *14*. https://doi.org/10.3390/app14020911.

 doi:10.20944/preprints202604.0925.v1

29. Ferrari, A.; Cutti, A.G.; Cappello, A. A new formulation of the coefficient of multiple correlation to assess the similarity of waveforms measured synchronously by different motion analysis protocols. *Gait & Posture* **2010**, *31*, 540–542. https://doi.org/10.1016/j.gaitpost.2010.02.009.
30. Brunyé, T.T.; Drew, T.; Kerr, K.F.; Shucard, H.; Powell, K.; Weaver, D.L.; Elmore, J.G. Zoom behavior during visual search modulates pupil diameter and reflects adaptive control states. *PloS One* **2023**, *18*, e0282616. https://doi.org/10.1371/journal.pone.0282616.
31. Strauch, C.; Wang, C.A.; Einhäuser, W.; Van der Stigchel, S.; Naber, M. Pupillometry as an integrated readout of distinct attentional networks. *Trends in Neurosciences* **2022**, *45*, 635–647. https://doi.org/10.1016/j.tins.2022.05.003.
32. Beatty, J. Task-evoked pupillary responses, processing load, and the structure of processing resources. *Psychological Bulletin* **1982**, *91*, 276–292. https://doi.org/10.1037/0033-2909.91.2.276.
33. Karpouzian-Rogers, T.; Sweeney, J.A.; Rubin, L.H.; McDowell, J.; Clementz, B.A.; Gershon, E.; Keshavan, M.S.; Pearlson, G.D.; Tamminga, C.A.; Reilly, J.L. Reduced task-evoked pupillary response in preparation for an executive cognitive control response among individuals across the psychosis spectrum. *Schizophrenia Research* **2022**, *248*, 79–88. https://doi.org/10.1016/j.schres.2022.07.018.
34. Yogev-Seligmann, G.; Hausdorff, J.M.; Giladi, N. The role of executive function and attention in gait. *Movement Disorders: Official Journal of the Movement Disorder Society* **2008**, *23*, 329–342; quiz 472. https://doi.org/10.1002/mds.21720.
35. Guertin, P.A. Central pattern generator for locomotion: anatomical, physiological, and pathophysiological considerations. *Frontiers in Neurology* **2012**, *3*, 183. https://doi.org/10.3389/fneur.2012.00183.
36. Shumway-Cook, A.; Woollacott, M.; Kerns, K.A.; Baldwin, M. The effects of two types of cognitive tasks on postural stability in older adults with and without a history of falls. *The Journals of Gerontology. Series A, Biological Sciences and Medical Sciences* **1997**, *52*, M232–240. https://doi.org/10.1093/gerona/52a.4.m232.
37. Al-Yahya, E.; Dawes, H.; Smith, L.; Dennis, A.; Howells, K.; Cockburn, J. Cognitive motor interference while walking: a systematic review and meta-analysis. *Neuroscience and Biobehavioral Reviews* **2011**, *35*, 715–728. https://doi.org/10.1016/j.neubiorev.2010.08.008.